



Title	X-ray Absorption Fine Structure (XAFS) Analysis of Titanium-implanted Soft Tissue
Author(s)	Uo, Motohiro; Asakura, Kiyotaka; Yokoyama, Atsuro; Ishikawa, Makoto; Tamura, Kazuchika; Totsuka, Yasunori; Akasaka, Tsukasa; Watari, Fumio
Citation	Dental Materials Journal, 26(2), 268-273
Issue Date	2007
Doc URL	http://hdl.handle.net/2115/20540
Rights	Copyright (C) 2007 Japanese Society for Dental Materials and Devices
Type	article (author version)
File Information	DMJ2007_XAFS_Analysis_of_Ti_implanted_Tissues.pdf



[Instructions for use](#)

X-ray Absorption Fine Structure (XAFS) Analysis of Titanium-implanted Soft Tissue

Motohiro UO¹, Kiyotaka ASAKURA², Atsuro YOKOYAMA³, Makoto ISHIKAWA⁴, Kazuchika TAMURA⁵, Yasunori TOTSUKA⁵, Tsukasa AKASAKA¹ and Fumio WATARI¹

¹Department of Biomedical Materials and Engineering, Graduate School of Dental Medicine, Hokkaido University, North 13, West 7, Kita-ku, Sapporo 060-8586, Japan

²Catalyst Research Center, Hokkaido University, North 21, West 10, Kita-ku, Sapporo 001-0021, Japan

³Department of Oral Functional Prosthodontics, Graduate School of Dental Medicine, Hokkaido University, North 13, West 7, Kita-ku, Sapporo 060-8586, Japan

⁴Department of Oral Diagnosis and Oral Medicine, Graduate School of Dental Medicine, Hokkaido University, North 13, West 7, Kita-ku, Sapporo 060-8586, Japan

⁵Department of Oral and Maxillofacial Surgery, Graduate School of Dental Medicine, Hokkaido University, North 13, West 7, Kita-ku, Sapporo 060-8586, Japan

Corresponding author: Motohiro UO

Running Title: XAFS analysis of titanium-implanted tissue

Keywords: X-ray absorption fine structure (XAFS), Titanium, Implant

SYNOPSIS

Tissues contacting Ti dental implants were subjected to X-ray absorption fine structure (XAFS) analysis to examine the chemical state of Ti transferred from the placed implant into the surrounding tissue. Nine tissues that contacted pure Ti cover screws for several months were excised in a second surgery whereby healing abutments were set. Six tissues that surrounded implants retrieved due to their failure were also excised. Ti distributions in the excised specimens were confirmed by X-ray scanning analytical microscopy (XSAM), and the specimens were subjected to fluorescence XAFS analysis to determine the chemical states of the low concentrations of Ti in the tissues surrounding Ti dental implants. Ti mostly existed in the metallic state and was considered to be debris derived from the abrasion of implant pieces during implant surgery. Oxidized forms of Ti, such as anatase and rutile, were also detected in a few specimens — and existed in either a pure state or mixed state with metallic Ti. It was concluded that the existence of Ti in the tissue did not cause implant failure. Moreover, the usefulness of XAFS for analysis of the chemical states of rarely contained elements in biological tissue was demonstrated.

INTRODUCTION

Metallic materials play an important role as medical and dental implants¹⁾. Indeed, base metal alloys (e.g., stainless steel, cobalt-chromium alloys, and titanium alloys) are widely used as major medical and dental materials for applications that require high mechanical strength. However, these base metal alloys contain metallic elements with low biocompatibility such as nickel and chromium, and erosion and mechanical wear of metal implants placed in the human body have been reported to be associated with localized and systemic problems²⁻⁶⁾.

Titanium (Ti) is one of the most chemically stable and biocompatible metals. Further, it induces osseointegration (direct bonding between bone and implant) and bone formation — both of which are important features for implants. However, even Ti erodes into the surrounding bone⁷⁻⁹⁾. Elemental distribution imaging using fluorescent X-rays — by virtue of its high sensitivity and low damage to specimens — has been employed to investigate heavy elements rarely contained in biological specimens¹⁰⁻¹³⁾. However, the chemical states of eroded metallic elements in the human body have not been reported because currently available conventional methods are merely able to detect seemingly unalarming, low concentrations — which are nonetheless significant enough to be assessed for biocompatibility.

X-ray absorption fine structure (XAFS) analysis is a useful method to reveal the chemical states of target elements. In particular, its use of synchrotron radiation makes it possible to analyze the state of eroded metal in the human body at low concentrations of around 1 to 100 ppm by using fluorescence XAFS^{14,15)}. In a previous study, we applied fluorescence XAFS to the analysis of human soft tissue in contact with Ti dental implants, and the chemical state of Ti in two oral mucosa specimens with low concentrations of Ti could be analyzed¹⁶⁾. In this study, 15 specimens from Ti dental implant-contacting tissues were analyzed by fluorescence XAFS to examine the chemical state of Ti transferred from the placed implant into the surrounding tissue.

MATERIALS AND METHODS

Tissue specimens

Fifteen oral mucosa specimens excised from nine patients through implant surgery were subjected to XAFS analysis. During dental implant surgery, fixtures of Brånemark[®] Mark III implants were inserted into the jaw bone. Each fixture was covered with a cover screw, and then both fixture and cover screw were submerged under the mucosa in the first surgery. Both the fixture and cover screw consisted of commercially pure Ti with machined surface.

Nine tissues that contacted the Ti cover were excised in a second surgery whereby healing abutments were set. These tissues had closely contacted the pure Ti for several months and were available as a result of the ordinary implantation process without a need for excess surgery. Six tissues that surrounded the tissues of implants retrieved due to their failure were also excised. The excised specimens were freeze-dried and subjected to XSAM and XAFS analyses. This study was carried out with the permission of the Ethical Committee of the Graduate School of Dental Medicine of Hokkaido University.

XSAM analysis

Ti and sulfur (S) distributions in the specimens were confirmed with an X-ray scanning analytical microscope (XSAM; XGT-2000V, Horiba). S was homogeneously contained in the specimens; therefore, S distribution images included the whole specimen. XSAM elemental distribution images were obtained with 50 scans (scan speed was 3,000 seconds per scan), and incident X-ray was obtained under the conditions of 50 kV, 1 mA. Resolution of XSAM was about 100 μm . Specimens that showed Ti localization by XSAM analysis were used for a subsequent XAFS analysis.

In a previous report¹³⁾ which also used XSAM, we observed clear Ni dissolution in Ni wire (99.9%, $\phi 1 \text{ mm} \times 10 \text{ mm}$)-implanted rat subcutaneous tissue. This tissue showed severe inflammatory responses such as cell necrosis, macrophage migration, and blood vessel dilation around the area with dissolved Ni¹³⁾. On this basis, it was also subjected to XAFS analysis as a negative control.

XAFS analysis

The XAFS spectra were measured at BL-9A of the Photon Factory, Institute of Materials Structure Science, High Energy Accelerator Organization (KEK-PF). Electron storage ring was operated at 2.5 GeV with 300–500 mA. Synchrotron radiation was monochromatized with a Si(111) double-crystal monochromator. Incident X-ray was focused using two bent conical mirrors into a beam 1 mm in diameter, and the specific area of the specimen where Ti was enriched was irradiated. Higher harmonics were removed using a total reflection mirror.

As for the X-ray absorption near edge structure (XANES) spectra of Ti K-edge and Ni K-edge, they were measured in a fluorescent mode using a multi-element solid-state detector (SSD; Camberra, 19 elements). I_0 signals were monitored using an N₂-filled ionization chamber. Ti foil (99.6%, Nilaco, Japan), Ni(NO₃)₂, and Ni(OH)₂ (reagent grade, Wako, Japan) were used as the standards for XAFS analysis. XANES spectra of TiO₂ (anatase and rutile) were taken from the report of Asakura *et al.*¹⁷⁾.

RESULTS

Table 1 shows the results of XAFS analysis of 15 specimens. Specimen Nos. 1 to 9 were derived from the oral mucosae in contact with the pure Ti cover screws through the second ordinary surgery. Specimen Nos. 10 to 15 were derived from the tissues surrounding retrieved implants. The chemical state of Ti was estimated by comparing the XANES spectra to those of reference compounds. Metallic Ti was mostly suggested; however, other states were also detected.

Figure 1 shows the typical S and Ti distribution images of four oral mucosae (numbers 1, 2, 4, and 7 in Table 1) with XSAM. The S distribution image shows the shape of the specimens. In these specimens, Ti was localized in spots, except in No. 2, suggesting the existence of particle-like materials consisting of Ti. In specimen No. 2, Ti was homogeneously distributed in parts of the specimen. Parts indicated by arrows in the Ti distribution images show the areas employed for subsequent XAFS analysis.

Figure 2 shows the Ti K-edge XANES spectra of specimen No. 1 (arrow in Fig. 1) and Ti foil as the standard. The spectrum of specimen No. 1 was quite close to that of Ti foil. Therefore, the localized Ti in specimen No. 1 was estimated to be in the metallic state.

Figure 3 shows the spectra of specimen No. 2 (as previously reported¹⁶⁾) and TiO₂ (anatase and rutile¹⁷⁾). The spectrum of specimen No. 2 was close to that of anatase. Therefore, the localized Ti in specimen No. 2 was considered to be anatase. Figure 4 shows the XANES spectrum of specimen No. 4. The observed XANES spectrum was similar to that of metallic Ti, but fit well with a mixture of metallic Ti and anatase. A mixture of about 80% metal and 20% anatase well described the observed spectrum. Figure 5 shows the XANES spectrum of specimen No. 7. Like specimen No. 4, the Ti distribution and the observed XANES spectrum indicated the presence of metallic Ti, but the peak marked by the arrow in the observed spectrum did not exist in the spectrum of metallic Ti. On the overall, the spectrum fit well with a mixture of metallic Ti (80%) and rutile (20%).

Figure 6 shows the Ni and S distribution images of Ni-implanted rat subcutaneous tissue obtained by XSAM. Ni dissolution was clearly observed, and the area with dissolved Ni extended up to about 1.5 mm from the position of the implant surface. The Ni K-edge XANES spectrum of the dissolved Ni in the abovementioned tissue and those of the standard Ni compounds are shown in Fig. 7. The spectrum of Ni dissolved in the rat soft tissue was close to that of Ni(OH)₂ and identical to that of Ni(NO₃)₂.

DISCUSSION

Despite the high chemical stability and biocompatibility of pure Ti dental implants, Ti was detected in tissues surrounding the implants. We analyzed 15 Ti-containing oral mucosae obtained from patients who had Ti dental implants, and the chemical state of Ti was estimated with fluorescence XAFS analysis. As shown in Table 1, 10 of the specimens showed the existence of metallic Ti. Further, as shown for specimen No. 1 in Fig. 1, the Ti distribution images of these specimens suggested the existence of particulate Ti. Putting these results together, it could be said that Ti in those tissues consisted of metallic Ti particles.

During the first implant surgery, the dental implant fixture was covered with a cover screw. The surface of placed implants in this study were machined but not polished. Therefore, abrasion between the inner surface of the fixture and the outer surface of the cover screw appeared to generate Ti debris. Wear debris generation from metal-on-metal hip joints *in vivo* has been reported¹⁸⁾. Therefore, the origin of Ti particles in these specimens was attributed to abrasion-generated debris during implant surgery. In the XSAM observation, Ca

distributions were also measured. These images were similar to S distribution images and there were no relations to Ti distribution images.

In one specimen (No. 2), Ti existed as anatase. In a few other specimens (Nos. 3, 4, 7, and 10), mixed states of metallic Ti and titanium dioxide (anatase or rutile) were observed. As shown for specimen Nos. 4 and 7 in Fig. 1, the Ti distribution images of these specimens suggested the existence of particulate Ti. Moreover, even in the mixed state, metallic Ti debris constituted a greater portion in these specimens with the existence of a small amount of anatase. One speculation for the origin of these oxides was that Ti eroded and dissolved into the surrounding tissue and might have oxidized and localized. Alternatively, the TiO₂ layer on the implant surface was abraded and transferred into the tissue. Anatase is the low-temperature form of titanium dioxide. As such, its presence as the oxidized state of dissolved Ti ions was a reasonable and acceptable one. Moreover, anatase formation from dissolved Ti can be corroborated from the many reports on the corrosion behavior of Ti^{19–28}. However, the existence of rutile was a curious one because it is a high-temperature form of titanium dioxide. One possible source was the abrasion of Ti oxide film on the implant material. In this case, the state of Ti would depend on the history and background of the material before surgery. Removed cover screws (specimen Nos. 1–9) and extracted implants (specimen Nos. 10–15) showed a metallic surface, whereby no corrosion was observed in visual inspection. On this note, the relationship between the chemical state of Ti in the surrounding tissues and the surface condition of implanted Ti was not fully clarified and thoroughly determined in this study. Additional study is thus necessary to confirm the transfer process of Ti.

The implants of six patients, specimen Nos. 1 to 9, were stable despite the transfer of Ti into the surrounding tissue. As shown in Table 1, the same chemical states were found for both successful and failed implants. In other words, implant failure could not be ascribed to the spread of Ti in the tissue. As for the explanation to this dual success/failure condition of implants, it could be attributed to two factors: Ti in the surrounding tissue was in a chemically stable state (such as metallic Ti and TiO₂), and that it was localized in a narrow area around the tissue in contact with the implant *versus* widespread dissemination of Ti debris from the implant.

In contrast to Ti, dissolved Ni spread homogeneously in the soft tissue and existed in an aquo complex as shown in Figs. 6 and 7. In the specimen shown in Fig. 6, severe

inflammatory responses such as cell necrosis, macrophage migration, and blood vessel dilation were observed in the area with dissolved Ni¹³). Figure 7 then suggested that the Ni species present in rat soft tissue was surrounded by water to form an aquo complex. The Ni aquo complex would be diffusible and reactive in the soft tissue. As a result, the toxicity of Ni ions caused severe inflammatory responses in the tissue. At this juncture, it is worth highlighting that differences in the chemical state between Ti and Ni in the soft tissue would affect the diffusibility and toxicity of dissolved species in the tissue. Therefore, analysis of the chemical state of a metal species in soft tissue was considered to be useful in evaluating its biocompatibility.

Concentrations of released metal ions and small debris in the tissues surrounding medical and dental implants are usually quite low. Therefore, such tissues require high-intensity incident X-rays (e.g., synchrotron radiation) coupled with high sensitivity (e.g., X-ray fluorescence or XAFS analysis). For example, Ektessabi *et al.*²⁹⁾ detected metal ions released from a failed hip replacement system by synchrotron radiation-excited X-ray fluorescence spectroscopy; however, their chemical states were still unknown. In this study, we employed fluorescence XAFS, which provided higher sensitivity than ordinary transmission XAFS with synchrotron radiation because of low background in the spectrum³⁰⁾. In this manner, the chemical states of low concentrations of metal elements in tissues were successfully analyzed using fluorescence XAFS method.

CONCLUSIONS

In this study, we successfully estimated the chemical states of low concentrations of Ti in tissues surrounding Ti dental implants using fluorescence XAFS. Ti existed mostly in the metallic state and was considered to be debris derived from the abrasion of implant pieces during implant surgery. Oxidized Ti forms, such as anatase and rutile, were also detected in a few specimens — they existed in either a pure state or mixed state with metallic Ti. As for Ti that transferred from the dental implants into the surrounding tissues, it existed in chemically stable states (such as metallic Ti and titanium dioxide) and localized near the implants. The same chemical states were found for both successful and failed implants, and always close to the implant surface. Therefore, failure could not be ascribed to the spreading of Ti in the tissue. In this work, we demonstrated the usefulness of using XAFS for the analysis of the chemical states of rarely contained metallic elements in tissues surrounding metallic implants.

ACKNOWLEDGEMENTS

The XAFS measurements were done with the approval of the Photon Factory Advisory Committee (Proposal No. 2004G084, 2006G199). This work was also supported by a Grant-in-Aid for Scientific Research (B), No. 18390509, from the Ministry of Education, Culture, Sports, Science and Technology, Japan.

REFERENCES

- 1) McNamara A, Williams DF. The response to the intramuscular implantation of pure metal. *Biomaterials* 1981; 2:33–40.
- 2) McNamara A, Williams DF. Scanning electron microscopy of the metal-tissue interface. I. Fixation methods and interpretation of results. *Biomaterials* 1982; 3:160–164.
- 3) McNamara A, Williams DF. Scanning electron microscopy of the metal-tissue interface. II. Observations with lead, copper, nickel, aluminum, and cobalt. *Biomaterials* 1982; 3:165–176.
- 4) Schliephake H, Reiss G, Urban R, Neukam FW, Guckel S. Metal release from titanium fixtures during placement in the mandible: An experimental study. *Int J Oral Maxillofac Implants* 1993; 8 502–511.
- 5) Hallab NJ, Skipor A, Jacobs JJ. Interfacial kinetics of titanium- and cobalt-based implant alloys in human serum: Metal release and biofilm formation. *J Biomed Mater Res* 2003; 65A:311–318.
- 6) Kasai Y, Iida R, Uchida A. Metal concentration in the serum and hair of patients with titanium alloy spinal implants. *Spine* 2003; 28:1320–1326.
- 7) Ferrari F, Miotello A, Pavloski L, Galvanetto E, Moschini G, Galassini S, Passi P, Bogdanovic S, Fazinic S, Jaksic M, Valkovic V. Metal-ion release from titanium and TiN coated implants in rat bone. *Nucl Instr and Meth B* 1993; B79:421–423.
- 8) Ektessabi AM, Otsuka T, Tsuboi Y, Yokoyama K, Albrektsson T, Sennerby L, Johansson C. Application of micro beam PIXE to detection of titanium ion release from dental and orthopaedic implants. *Int J PIXE* 1994; 4:81–91.
- 9) Gorustovich A, Rosenbusch M, Guglielmotti MB. Characterization of bone around titanium implants and bioactive glass particles: an experimental study in rats. *Int J Oral Maxillofac Implants* 2002; 17:644–650.
- 10) Kitamura N, Ektessabi AM. XAFS in a single macrophage cell. *J Synchrotron Rad* 2001; 8:981–983.
- 11) Kagoshima Y, Takai K, Ibuki T, Yokoyama Y, Hashida T, Yokoyama K, Takeda S, Urakawa M, Miyamoto N, Tsusaka Y, Matsui J, Aino M. Scanning hard X-ray microscope with tantalum phase zone plate at the Hyogo-BL (BL24XU) of SPring-8. *Nucl. Instrum & Methods A* 2001; 467–468:872–876.
- 12) Dillon CT, Kennedy BJ, Lay PA, Lai B, Cai Z, Stampfl APJ, Ilinski P, Legnini DG, Maser J, Rodrigues W, Shear-McCarthy G, Cholewa M. Implementation of X-ray microscopy and micro-XANES analysis for investigations of the cellular uptake and cellular metabolism of transition metals. *J Phys IV* 2003; 104:293–296.
- 13) Uo M, Tanaka M, Watari F. Quantitative analysis of biological specimens by X-ray scanning analytical microscopy. *J Biomed Mater Res B Appl Biomater* 2004; 70B:146–151.
- 14) Nomura M. Dead-time correction of a multi-element SSD for fluorescent XAFS. *J Synchrotron Rad* 1998; 5:851–853.
- 15) Chun WJ, Tanizawa Y, Shido T, Iwasawa Y, Nomura M, Asakura K. Development of an in situ polarization-dependent total-reflection fluorescence XAFS measurement system. *J Synchrotron Rad* 2001; 8:168–172.
- 16) Uo M, Asakura K, Yokoyama A, Tamura K, Totsuka Y, Akasaka T, Watari F. Analysis of titanium dental implants surrounding soft tissue using X-ray absorption fine structure (XAFS) analysis. *Chem Lett* 2005; 34:776–777.
- 17) Asakura K, Inukai J, Iwasawa Y. Structure of one atomic layer titanium oxide on silica and its palladium-mediated restructuring. *J Phys Chem* 1992; 96:829–834.
- 18) Büscher R, Täger G, Dudzinski W, Gleising B, Wimmer MA, Fischer A. Subsurface microstructure of metal-on-metal hip joints and its relationship to wear particle generation. *J Biomed Mater Res Part B* 2005; 72B:206–214.
- 19) Khan MA, Williams RL, Williams DF. *In-vitro* corrosion and wear of titanium alloys in the biological environment. *Biomaterials* 1996; 17:2117–2126.

- 20) Cai Z, Nakajima H, Woldu M, Berglund A, Bergman M, Okabe T. *In vitro* corrosion resistance of titanium made using different fabrication methods. *Biomaterials* 1999; 20:183–190.
- 21) Grosgeat B, Reclaru L, Lissac M, Dalard F. Measurement and evaluation of galvanic corrosion between titanium/Ti6Al4V implants and dental alloys by electrochemical techniques and auger spectrometry. *Biomaterials* 1999; 20:933–941.
- 22) Nakagawa M, Matsuya S, Udoh K. Corrosion behavior of pure titanium and titanium alloys in fluoride containing solutions. *Dent Mater J* 2001; 20:305–314.
- 23) Hanawa T, Hiromoto S, Asami K, Okuno O, Asaoka K. Surface oxide films on titanium alloys regenerated in Hanks' solution. *Mater Trans* 2002; 43:3000–3004.
- 24) Cai Z, Shafer T, Watanabe I, Nunn ME, Okabe T. Electrochemical characterization of cast titanium alloys. *Biomaterials* 2003; 24:213–218.
- 25) Takahashi M, Kikuchi M, Takada Y, Okuno O, Okabe T. Corrosion behavior and microstructures of experimental Ti-Au alloys. *Dent Mater J* 2004; 23:109–116.
- 26) Takemoto S, Hattori M, Yoshinari M, Kawada E, Asami K, Oda Y. Corrosion behavior and surface characterization of Ti-20Cr alloy in a solution containing fluoride. *Dent Mater J* 2004; 23:379–386.
- 27) Takada Y, Okuno O. Corrosion characteristics of α -Ti and Ti₂Cu composing Ti-Cu alloys. *Dent Mater J* 2005; 25:610–616.
- 28) Matono Y, Nakagawa M, Matsuya S, Ishikawa K, Terada Y. Corrosion behavior of pure titanium and titanium alloys in various concentrations of Acidulated Phosphate Fluoride (APF) solutions. *Dent Mater J* 2006; 25:104–112.
- 29) Ektessabi AM, Rokkum M, Johansson C, Albrektsson T, Sennerby L, Saisho H, Honda S. Application of synchrotron radiation in investigation of metal-ion release from a hip replacement prosthesis. *J Synchrotron Rad* 1998; 5:1136–1138.
- 30) Asakura K. Fluorescent XAFS. *Shokubai* 2000; 42:328–332.

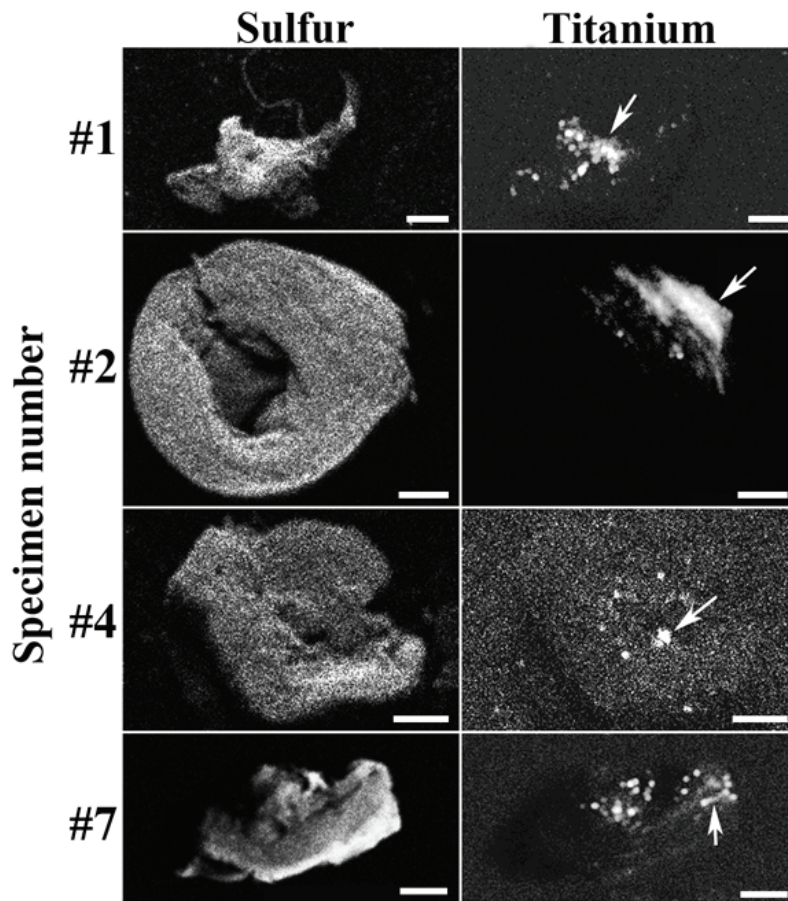


Figure 1 Elemental distribution images of typical Ti implant-surrounding tissues using XSAM (bars in images show 1 mm).

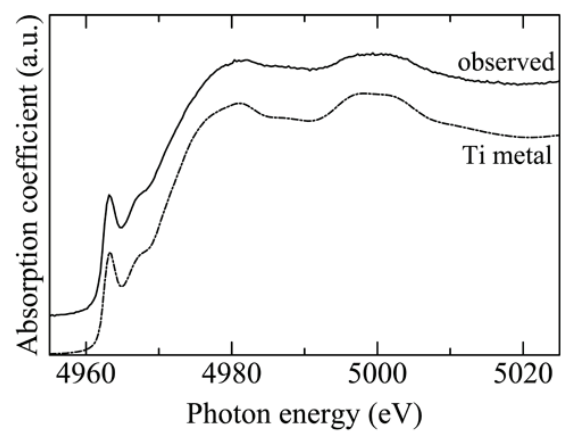


Figure 2 Ti K-edge XANES spectra of specimen No. 1 and Ti foil.

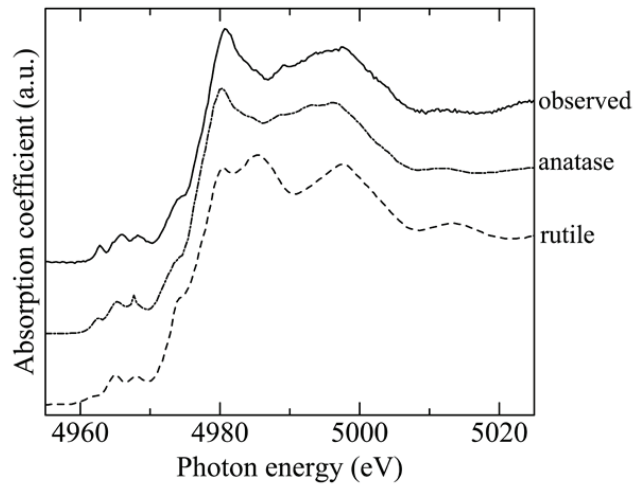


Figure 3 Ti K-edge XANES spectra of specimen No. 2 and TiO₂ in rutile and anatase forms after Asakura *et al.*¹⁷⁾.

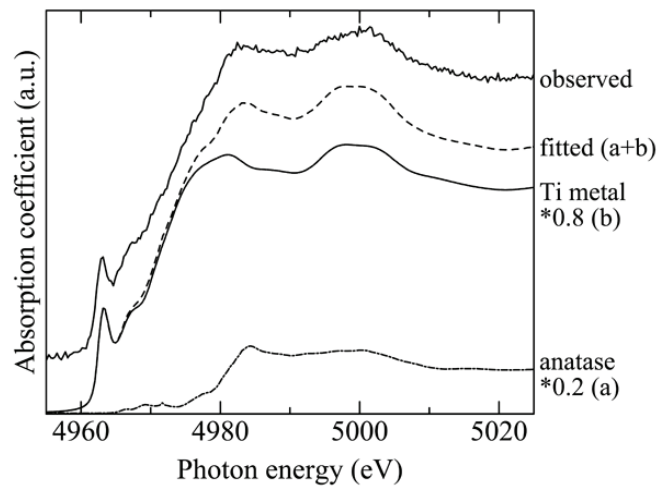


Figure 4 Ti K-edge XANES spectrum of specimen No. 4 and a curve fitting those of metallic Ti and TiO₂ in anatase.

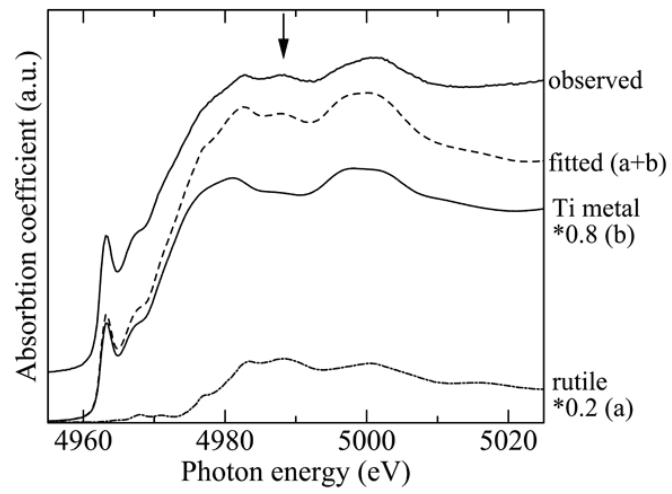


Figure 5 Ti K-edge XANES spectrum of specimen No. 7 and a curve fitting those of metallic Ti and TiO₂ in rutile.

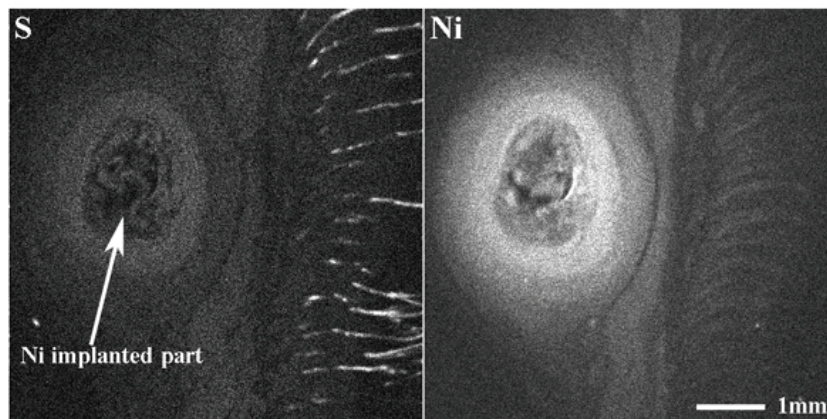


Figure 6 Elemental distribution images of Ni-implanted rat subcutaneous tissue using XSAM.

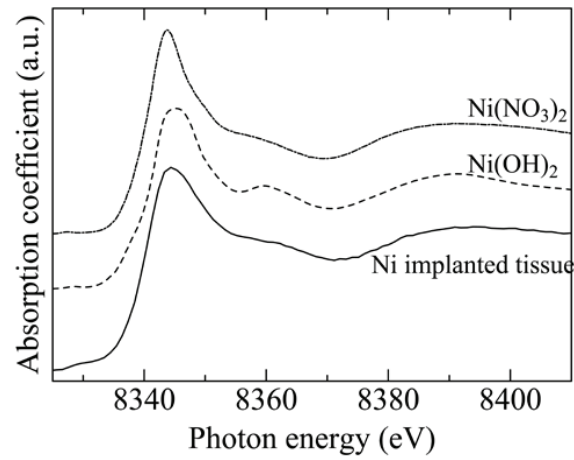


Figure 7 Ni K-edge XANES spectrum of an Ni-implanted rat specimen and those of $\text{Ni}(\text{NO}_3)_2$ and $\text{Ni}(\text{OH})_2$.

Table 1 Ti K-edge absorption and chemical state of Ti contained in Ti implant (Brånemark® Mark III)-surrounding tissues using fluorescence XAFS analysis. (Nos. 1 to 9: in contact with pure Ti cover screws (machined surface) of successful implants; Nos. 10 to 15: excised from retrieved implants with machined surface.)

Specimen	Chemical state of Ti	Patient (Gender)
1	Metal	A (Female)
2	Anatase	B (Female)
3	Metal (80%) + Anatase (20%)	B (Female)
4	Metal (80%) + Anatase (20%)	C (Female)
5	Metal	D (Female)
6	Metal	D (Female)
7	Metal (80%) + Rutile (20%)	E (Male)
8	Metal	E (Male)
9	Metal	F (Male)

10	Metal (85%) + Anatase (15%)	E (Male)
11	Metal	E (Male)
12	Metal	G (Female)
13	Metal	G (Female)
14	Metal	G (Female)
15	Metal	G (Female)